

available at www.sciencedirect.comjournal homepage: www.ejconline.com

Antisense treatment of IGF-IR induces apoptosis and enhances chemosensitivity in central nervous system atypical teratoid/rhabdoid tumours cells

J. D'cunja^a, T. Shalaby^a, P. Rivera^a, A. von Büren^a, R. Patti^b, F.L. Heppner^c,
A. Arcaro^d, L.B. Rorke-Adams^e, P.C. Phillips^b, M.A. Grotzer^{a,*}

^aNeuro-Oncology Program, University Children's Hospital of Zurich, Steinwiesstrasse 75, CH-8032 Zurich, Switzerland

^bDivision of Oncology, The Children's Hospital of Philadelphia, Philadelphia, PA, USA

^cInstitute of Neuropathology, University Hospital Zurich, University of Zurich, Switzerland

^dClinical Chemistry and Biochemistry, University Children's Hospital of Zurich, Switzerland

^eDepartment of Pathology, The Children's Hospital of Philadelphia, Philadelphia, PA, USA

ARTICLE INFO

Article history:

Received 3 August 2006

Received in revised form 28

November 2006

Accepted 5 March 2007

Available online 18 April 2007

Keywords:

Brain tumours

Novel therapies

Antisense oligonucleotide

Rhabdoid tumour

ABSTRACT

Central nervous system (CNS) atypical teratoid/rhabdoid tumours (AT/RT) are among the paediatric malignant tumours with the worst prognosis and fatal outcome. Insulin-like growth factor I receptor (IGF-IR) protects cancer cells from apoptosis induced by a variety of anticancer drugs and radiation. In the present study, IGF-IR was expressed in 8/8 primary AT/RT as detected by immunohistochemistry. Moreover, we found IGF-I and IGF-II mRNA in BT-16 CNS AT/RT cells and IGF-II mRNA in BT-12 CNS AT/RT cells, and autophosphorylated IGF-IR in both cell lines, indicating the potential presence of an autocrine/paracrine IGF-I/II/IGF-IR loop in CNS AT/RT. IGF-IR antisense oligonucleotide treatment of human CNS AT/RT cells resulted in significant down-regulation of IGF-IR mRNA and protein expression, induction of apoptosis, and chemosensitisation to doxorubicin and cisplatin. These studies provide evidence for the influence of IGF-IR on cellular responses to chemotherapy and raise the possibility that curability of selected CNS AT/RT may be improved by pharmaceutical strategies directed towards the IGF-IR.

© 2007 Elsevier Ltd. All rights reserved.

1. Introduction

Central nervous system (CNS) atypical teratoid/rhabdoid tumour (AT/RT) is a highly malignant embryonal tumour in young children. CNS AT/RT is characterised by the presence of rhabdoid cells, with or without fields resembling classical primitive neuroectodermal tumour (PNET), epithelial tissue and neoplastic mesenchyme.¹ The unique clinical, biological and histological features of this tumour have been defined over the past decade.^{2,3} It is similar to the renal malignant

rhabdoid tumour of infancy in its aggressiveness, in some histological features and in the loss of function of hSNF5/INI1, a recently described candidate tumour suppressor gene on chromosome 22.⁴ Experience to date indicates that infants and children with CNS AT/RT respond very poorly to chemotherapy and radiotherapy.^{5–8} In one of the largest reported series of patients with primary CNS AT/RT, only 6 of 36 children who received chemotherapy showed objective responses (>50% reduction in tumour mass) to chemotherapy and only 2 of 10 patients showed objective responses to radiotherapy.¹

* Corresponding author: Tel.: +41 44 266 7111; fax: +41 44 266 7171.

E-mail address: Michael.Grotzer@kispi.unizh.ch (M.A. Grotzer).
0959-8049/\$ - see front matter © 2007 Elsevier Ltd. All rights reserved.
doi:10.1016/j.ejca.2007.03.003

The median time to clinical progression was 4.5 months and the median overall survival was 6 months. More recently, aggressive therapy including high-dose chemotherapy with stem cell rescue and intrathecal chemotherapy has prolonged the natural history in a subset of children.⁷ However, the prognosis for children presenting with CNS AT/RT before the age of 3 years is still dismal.^{7,8} To date, there are no explanations for the remarkable resistance of this particular tumour to cytostatic drugs and radiotherapy.

Insulin-like growth factor I receptor (IGF-IR) plays a fundamental role in cell growth and malignant transformation and is an important mediator of antiapoptotic signals.^{9,10} IGF-IR is a membrane-bound heterotetramer receptor with two extracellular ligand-binding α -subunits and two transmembrane β -subunits with intrinsic tyrosine kinase activity. It is highly expressed in a variety of human tumours including malignant gliomas, meningiomas and medulloblastoma.^{11–14} Ogino et al. analysed two primary AT/RT by immunohistochemistry and demonstrated strong positivity for IGF-IR and one of its ligands (IGF-II), supporting the hypothesis that autocrine/paracrine stimulation of cell growth by IGF-IR might be involved in AT/RT tumorigenesis.¹⁵ Experiments using dominant negative mutants of IGF-IR, antibodies to IGF-IR, or antisense strategies directed against IGF-IR mRNA have shown that decreased or aberrant receptor expression is associated with a reversal of the transformed phenotype, induction of apoptosis and decrease of cellular radioresistance- and chemoresistance.^{16–19} Hence, IGF-IR has qualified as a target for the development of novel anti-cancer therapies in selected tumour types.^{16,20}

In this study, we evaluated IGF-IR expression in primary CNS AT/RT and compared it to near-normal brain samples and other paediatric brain tumours. In two human CNS AT/RT cell lines, expression of IGF-IR, IGF-I and IGF-II was determined to study possible autocrine/paracrine loops. Moreover, we down-regulated IGF-IR in two human CNS AT/RT cell lines using an antisense oligonucleotide approach and measured proliferation, apoptosis and chemosensitivity.

2. Patients and methods

2.1. Primary tumour samples

Formalin-fixed, paraffin-embedded CNS AT/RT samples for performing immunohistochemistry were available from 8 CNS AT/RT patients treated at The Children's Hospital of Philadelphia, PA. The median age at diagnosis of these CNS AT/RT patients was 4.0 years (range 0.8–10.0 years); 6 were male and 2 were female. Tumour location was infratentorial in 5 patients and supratentorial in 3 patients. Snap frozen tumour samples for performing Western blotting were available from 2 CNS AT/RT (left frontal lobe, male, 5.1 years; cerebellum, male, 10.0 years), 17 medulloblastoma, 2 glioblastoma, 2 anaplastic astrocytoma, and 4 pilocytic astrocytoma patients treated at The Children's Hospital of Philadelphia, PA. Near-normal brain samples included cerebellum of a 4-year-old glioma patient, temporal cortex from a 4-year-old epilepsy surgery patient, temporal cortex from a 14-year-old epilepsy surgery patient, and occipital cortex from a 19-year-old epilepsy surgery patient. Tumour and near-normal brain sam-

ples were snap frozen in liquid nitrogen in the operating room and then stored at -80°C until further analysis.

2.2. Human CNS AT/RT cells

BT-12 and BT-16 human CNS AT/RT cells were kind gifts from Dr. Jaclyn Biegel, The Children's Hospital of Philadelphia, PA. These cell lines have been established from two infants with CNS AT/RT (BT-12 from a 6-week-old female; BT-16 from a 2-year-old male). They have been analysed for INI1 mutations by Dr. Jaclyn Biegel and both contain INI1 mutations. BT-12 and BT-16 cells were cultured in DMEM (with Glutamax)/10% FBS. All cell cultures were maintained at 37°C in a humidified atmosphere with 5% CO_2 .

2.3. Immunohistochemistry

For histology, tissues were processed according to standard protocols and stained with haematoxylin-eosin (HE). Immunohistochemical stains were carried out on an automated Nexus staining apparatus (Ventana Medical Systems), following the manufacturer's guidelines. Antibodies to glial fibrillary protein (GFAP; 1:300; Dako), INI1 (BAF47; 1:100, BD Biosciences), alpha-smooth muscle actin (SMA; 1:20,000, Sigma) and epithelial membrane antigen (EMA; 1:20; Dako) were used.

For IGF-IR immunostaining, sections were deparaffinised with xylene, rehydrated and then blocked with 1% hydrogen peroxide in methanol. After pretreatment with microwaves (15 min in dH_2O) and washing with 0.1 M Tris and 2% horse serum, the slides were incubated overnight with a polyclonal IGF-IR β antibody (Santa Cruz Biotechnology, Santa Cruz, CA; Ref. [13]) at a 1:500 dilution. To detect the reaction, the slides were incubated for 60 min with a goat anti-rabbit biotinylated antibody (Vector Laboratories, Burlington, CA) at a 1:500 dilution and horseradish peroxidase StreptAvidin (Vector Laboratories, Burlington, CA) at a 1:1000 dilution. The immune complex was visualised with the chromogenic substrate diaminobenzidine tetrahydrochloride. For all samples, negative controls included omission of primary antibody and pre-absorption of the primary antibody with IGF-IR β -blocking peptide (Santa Cruz Biotechnology, Santa Cruz, CA). Normal human cerebellum was used as a positive control.

2.4. Western blot analysis

For protein analysis, cells growing in their mid-log phase, homogenised frozen tumour, and near-normal brain tissue samples were prepared in the lysis buffer (HEPES, pH 7.6: 25 mM; Triton X-100: 0.1%; NaCl: 300 mM; β -glycerophosphate: 20 mM; MgCl_2 : 1.5 mM; EDTA: 0.2 mM; DTT: 2 M; sodium orthovanadate: 0.2 mM; sodium fluoride: 10 mM; benzamide: 1 mM; leupeptin: 2 $\mu\text{g}/\text{ml}$; aprotinin: 4 $\mu\text{g}/\text{ml}$ and PMSF: 500 μM) and incubated on ice for 30 min. The lysate was centrifuged at 10,000g for 30 min and the supernatants were stored at -80°C until further use. After estimating the protein concentration by the BCA method (Pierce), the lysates were electrophoresed on SDS-polyacrylamide gels, and the gels were subjected to immunoblotting. Membranes were incubated overnight at 4°C with anti-IGF-IR β polyclonal antibody (Santa Cruz Biotechnology, Heidelberg, Germany), or

anti- β -actin monoclonal antibody (Abcam Ltd., Cambridge, UK). Membranes were then washed three times at room temperature and bound Ig was detected with anti-isotype monoclonal antibody coupled to horseradish peroxidase (Santa Cruz Biotechnology, Santa Cruz, CA). The signal was visualised by enhanced chemiluminescence ECL (Amersham Biosciences, Dübendorf, Switzerland) and autoradiography. For densitometry, the zymographic profiles of the gels were scanned and densitometry performed by using NIH Image-Quant. IGF-IR expression was semi-quantitated by comparison with the profiles of the near-normal brain samples.

Immunoprecipitations were performed using 1 μ g of IGF-IR β antibody per 100 μ g of protein lysate. After incubation at 4 °C for 2 h, the complex was precipitated with protein A Sepharose, electrophoresed on 8% polyacrylamide gels, and transferred on to a nitrocellulose membrane. The blot was then probed with a phosphotyrosine-specific antibody (PY99; Santa Cruz Biotechnology, Santa Cruz, CA).

2.5. Quantitative RT-PCR

Isolation of total RNA and cDNA synthesis were performed as previously described.²¹ Quantitative RT-PCR of IGF-IR, IGF-I and IGF-II mRNA was performed using an ABI Prism 7700 Sequence Detection System (Applied Biosystems, Rotkreuz, Switzerland), as described.²² Primers and probes for IGF-IR, IGF-I, IGF-II, and the endogenous control 18S rRNA were purchased from Microsynth (Balgach, Switzerland). For primers and probes sequences, see Table 1. Experiments were performed in triplicate for each data point. Each sample was normalised on the basis of its 18S rRNA content.

2.6. Uptake of IGF-IR antisense oligonucleotides to CNS AT/RT cells

Antisense phosphorothioate oligonucleotides directed against IGF-IR and control scrambled IGF-IR oligonucleotides with a similar base composition but a randomised sequence as a control were designed and manufactured by Biognostik (Göttingen, Germany). Fluorescein-labelled phosphorothioate oligonucleotides were used to monitor cellular uptake. Exponentially growing BT-12 and BT-16 human CNS AT/RT

cells were plated in 16-well plastic chamber slides (Biognostik, Göttingen, Germany) (2×10^3 cells/well) and 2 μ M fluorescein-labelled phosphorothioate oligonucleotides were directly added into the wells. Cells were fixed after 8, 12, 24, and 48 h with -20 °C methanol and slides were sealed with mounting medium containing 4,6-diamidino-2-phenylindole (Vectashield Vector Laboratories, Burlingame, CA). Fluorescent uptake and distribution was visualised by fluorescence microscopy. To determine the percentage of uptake, FITC-labelled cells were counted and related to the total number of cells as previously described.²³

2.7. Measurement of cell viability

Exponentially growing BT-12 and BT-16 human CNS AT/RT cells (3×10^3 cells/well) were treated with 2 μ M IGF-IR antisense oligonucleotides for 0, 8, 12, 24, 48, 72, and 96 h. Controls included untreated cells, and cells treated with scrambled oligonucleotides. A colourimetric 3-(4,5-dimethylthiazol-2-yl)-5-(3-carboxymethoxyphenyl)-2-(4-sulphophenyl)-2H-tetrazolium, inner salt (MTS) assay (Promega, Wallisellen, Switzerland) was used to quantitate cell viability as previously described.²⁴ Each condition was performed in triplicate.

2.8. Detection of apoptosis

Exponentially growing BT-12 and BT-16 cells (3×10^3 cells/well) were incubated with 2 μ M IGF-IR antisense oligonucleotides for 0, 24, 48, 72 and 96 h. Controls included untreated cells, and cells treated with scrambled oligonucleotides. A photometric enzyme-immunoassay (Cell Death Detection ELISA^{PLUS}; Roche Diagnostics, Basel, Switzerland) was used for the quantitative determination of cytoplasmic histone-associated DNA fragments, as described previously.²⁴

2.9. Treatment of IGF-IR antisense pretreated CNS AT/RT cells with cytotoxic drugs

After 24 h pretreatment with IGF-IR antisense oligonucleotides (2 μ M), BT-12 and BT-16 human CNS AT/RT cells (3×10^3 cells/well) were treated with cisplatin or doxorubicin in the concentrations indicated. After a further incubation of 48 h, cell viability was quantified by the MTS assay. Controls included cells pretreated with scrambled oligonucleotides and cells without pretreatment.

2.10. Statistical analysis

GraphPad Prism 4 (GraphPad Software, San Diego, CA, USA) software was used to calculate IC₅₀ values and their 95% confidence intervals and to compare the fitted midpoints (log IC₅₀) of the two curves statistically.

Table 1 – Sequences of primers and probes used for quantitative RT-PCR

Gene	Sequence of primers and probes
IGF-I	Forward 5'-AAGTCAGCTCGCTCTGTCCG-3' Reverse 5'-TTCCTGCACTCCCTCTACTTGC-3' Probe 5'-TCTGGGTCTTGGGCATGTCGGTGT-3'
IGF-II	Forward 5'-ACGTTCACTCTGTCTCTCCCACTA-3' Reverse 5'-AATT CGTCTGATTGTCCAGGGAGG-3' Probe 5'-ACAGCTGACCTCATTTCCT GATACCT-3'
IGF-IR	Forward 5'-GTGAAAGTGACGTCCTGCATTTC-3' Reverse 5'-CCTTGTAGTAAACGGTGAAGCTGA-3' Probe 5'-CACCACCACTGCGAAGAATCGCATC-3'
18S rRNA	Forward 5'-AGTCCCTGCCCTTTGTACACA-3' Reverse 5'-GATCCGAGGGCTCACTAAAC-3' Probe 5'-CGCCCGTCGCTACTACCGATTGG-3'

3. Results

3.1. Expression of IGF-IR in primary CNS AT/RT

To study the expression of IGF-IR in CNS AT/RT, we performed immunohistochemistry in eight formalin-fixed,

paraffin-embedded primary CNS AT/RT and found IGF-IR expression in all tumours studied (Fig. 1). For comparative quantification, we performed Western blotting with a polyclonal IGF-IR β chain antibody in frozen tumour samples of 2 CNS AT/RT, 18 medulloblastoma, 8 glial tumours and 4 near-normal brain samples. We found a clear IGF-IR overexpression in CNS AT/RT compared to near-normal brain samples (Fig. 2a) and high IGF-IR expression in CNS AT/RT compared to medulloblastoma and paediatric glial CNS tumours (Fig. 2b).

3.2. IGF-I and IGF-II expression in human CNS AT/RT cells

To study the functional activity of IGF-IR and possible auto-crine/paracrine loops, we performed Western blotting, autophosphorylation studies and RT-PCR for IGF-I and IGF-II in two human CNS AT/RT cell lines (Table 2). In BT-16 CNS AT/RT cells, high levels of autophosphorylated IGF-IR and expression of IGF-I and IGF-II mRNA were detected indicating a possible autocrine/paracrine loop. In BT-12 cells, IGF-IR protein expression was lower when compared to BT-16 cells, and no

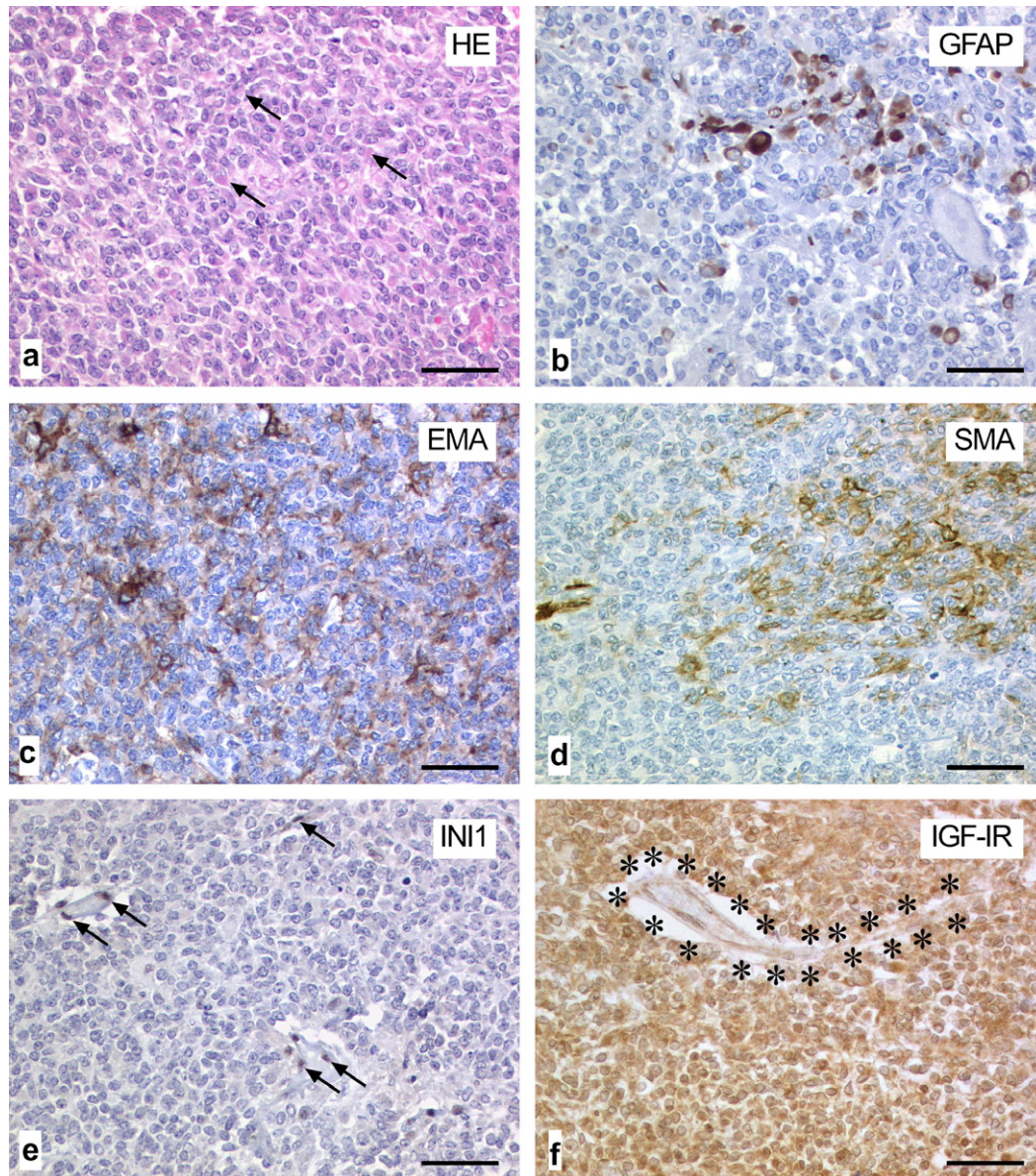


Fig. 1 – Exemplary morphological and immunohistochemical appearance of one out of eight investigated primary CNS AT/RT: depicted is a malignant, highly cellular tumour consisting of numerous rhabdoid cells (arrows; hematoxylin and eosin, HE; a). Immunohistochemical stainings revealed areas of epithelial, mesenchymal and neuroectodermal differentiation as demonstrated by focal positivity for glial fibrillary acidic protein (GFAP, b), epithelial membrane antigen (EMA, c), smooth muscle actin (SMA, d). As reported for the majority of AT/RTs, INI1 protein expression was lacking (internal positive control: endothelial cells, arrows; e), probably due to inactivation of the *INI1/hSNF5* gene. Virtually all tumour cells displayed a strong immunoreactivity for IGF-IR (internal negative control: endothelial cells of a vessel (asterisks), which, at best, exhibited a slight background signal, f). Scale bars: a–f: 50 μ m.

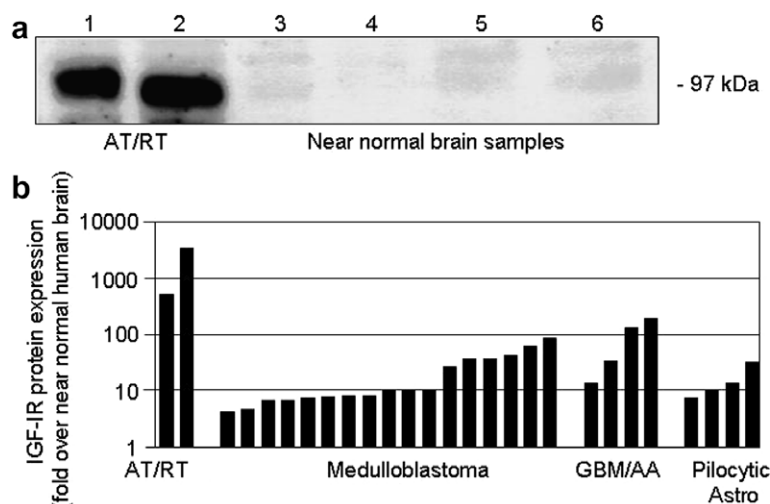


Fig. 2 – (a) Western blot analysis demonstrating high IGF-IR protein expression in primary CNS AT/RT (lanes 1 and 2) compared to near-normal brain samples (lanes 3–6). Protein samples (100 µg) were electrophoresed on 8% SDS gels, transferred to Immobilon-P membrane, and probed with IGF-IR β chain (97 kDa) antibodies. (b) Densitometric quantitation of IGF-IR protein expression in two primary CNS AT/RT compared to other childhood brain tumours (17 medulloblastoma, four high-grade gliomas and four pilocytic astrocytomas). Tumour tissue lysates (100 µg protein) were analysed for the expression of IGF-IR by Western blot analysis.

Table 2 – Characteristics of BT-12 and BT-16 human CNS AT/RT cells

	IGF-IR protein (Western blotting)	IGF-IR autophosphorylation (Immunoprecipitation, phosphotyrosin Ab)	IGF-I mRNA (RT-PCR)	IGF-II mRNA (RT-PCR)
BT-12	+	+	–	+
BT-16	+++	+++	+	++
+++; high expression; ++; medium expression; +; low expression; –; no expression detectable.				

IGF-I, but IGF-II was detectable. IGF-IR was also found to be autophosphorylated, but to a lesser extent than in BT-16 cells.

3.3. Antisense oligonucleotide-mediated down-regulation of IGF-IR mRNA and protein expression

Uptake of the IGF-IR antisense oligonucleotides into the CNS AT/RT cells was monitored using fluorescein-labelled oligonucleotides. A maximal uptake of 70–80% was reached with a concentration of 2 µM after 12 h treatment in three independent experiments. This level was kept for 24 and 48 h after treatment. Increasing the amount of antisense molecules and incubation for longer times generated no increase in oligonucleotide uptake. We then treated BT-12 and BT-16 human CNS AT/RT cells for 48 h with IGF-IR antisense oligonucleotides (2 µM) and determined IGF-IR mRNA expression by quantitative RT-PCR and IGF-IR protein expression by Western blotting. In IGF-IR antisense oligonucleotide-treated BT-12 (BT-16) cells, the mean IGF-IR mRNA expression levels were reduced to 51% (61%) compared to untreated cells and to 59% (75%) compared to control cells treated with scrambled oligonucleotides (Fig. 3a). In IGF-IR antisense oligonucleotide-treated BT-12 (BT-16) cells, the mean IGF-IR protein expression levels were reduced to 39% (47%) compared to un-

treated cells and to 53% (51%) compared to control cells treated with scrambled oligonucleotides (Fig. 3b).

3.4. IGF-IR antisense treatment suppresses CNS AT/RT cell proliferation

Treatment of BT-12 and BT-16 human CNS AT/RT cells with IGF-IR antisense oligonucleotides (2 µM) resulted in a significant time-dependent decrease of cellular proliferation when compared to untreated and scrambled oligonucleotide-treated cells as determined by the MTS assay (Fig. 4). No significant differences in cellular proliferation were detected between untreated or scrambled oligonucleotide-treated cells.

3.5. IGF-IR antisense treatment increases apoptotic cell death in CNS AT/RT cells

Treatment of BT-12 and BT-16 CNS AT/RT cells with IGF-IR antisense oligonucleotides (2 µM) resulted in a significant time-dependent increase of apoptotic cell death when compared to untreated and scrambled oligonucleotide-treated cells, as determined by Cell Death ELISA (Fig. 5). There were no significant differences in apoptotic cell death between untreated or scrambled oligonucleotide-treated cells.

3.6. IGF-IR antisense treatment sensitises CNS AT/RT cells to chemotherapy

To investigate whether IGF-IR down-regulation alters chemosensitivity in CNS AT/RT cells, we tested different cytotoxic drugs (doxorubicin, cisplatin) in IGF-IR antisense oligonucleotide pretreated (2 μ M; 24 h) BT-12 and BT-16 human CNS AT/

RT cells, and measured cell proliferation by MTS assay. For the two cytotoxic drugs tested, BT-16 human CNS AT/RT cells were less sensitive when compared to BT-12 cells. We then compared chemosensitivity of IGF-IR antisense oligonucleotide treated cells with scrambled oligonucleotide treated control cells. As shown in Fig. 6, IGF-IR down-regulation by antisense oligonucleotides resulted in significant increases

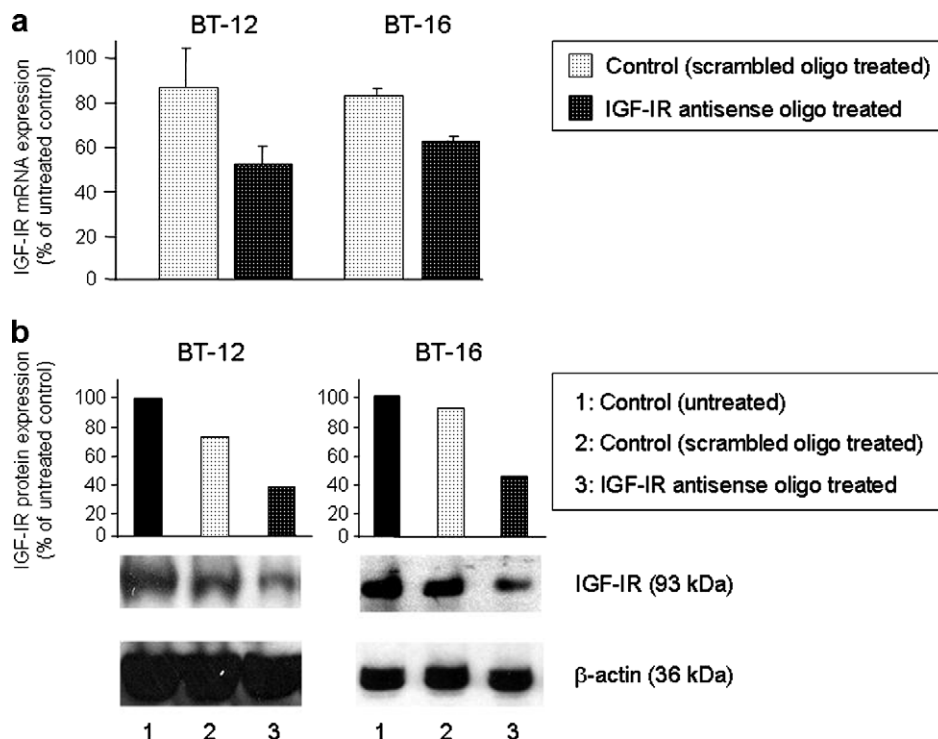


Fig. 3 – Down-regulation of IGF-IR mRNA (a) and protein expression (b) by IGF-IR antisense oligonucleotide treatment (2 μ M; 48 h) in human CNS AT/RT cells, as measured by quantitative RT-PCR (values represent the mean expression + SD $n = 3$) and Western blot analysis (representative example).

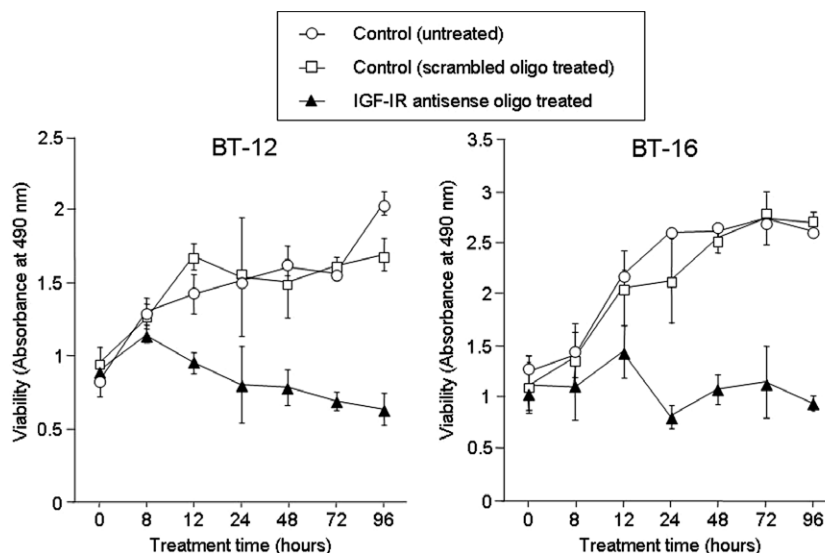


Fig. 4 – Down-regulation of IGF-IR through antisense oligonucleotide treatment (2 μ M) suppresses proliferation in BT-12 and BT-16 human CNS AT/RT cells, as measured by MTS assay at different time points. Values represent the absorbance at 490 nm \pm SD ($n = 3$).

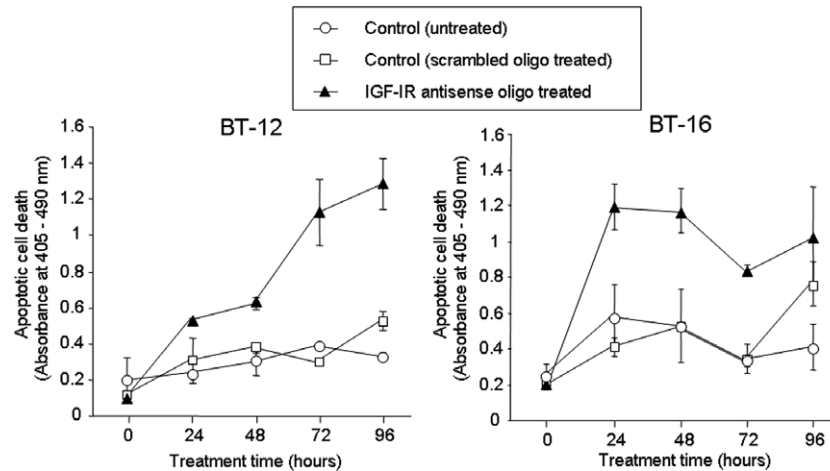


Fig. 5 – Down-regulation of IGF-IR through antisense oligonucleotide treatment (2 μ M) increases apoptotic cell death in BT-12 and BT-16 human CNS AT/RT cells, as measured by Cell Death ELISA at different time points. Values represent the absorbance at (405–490 nm) \pm SD ($n = 3$).

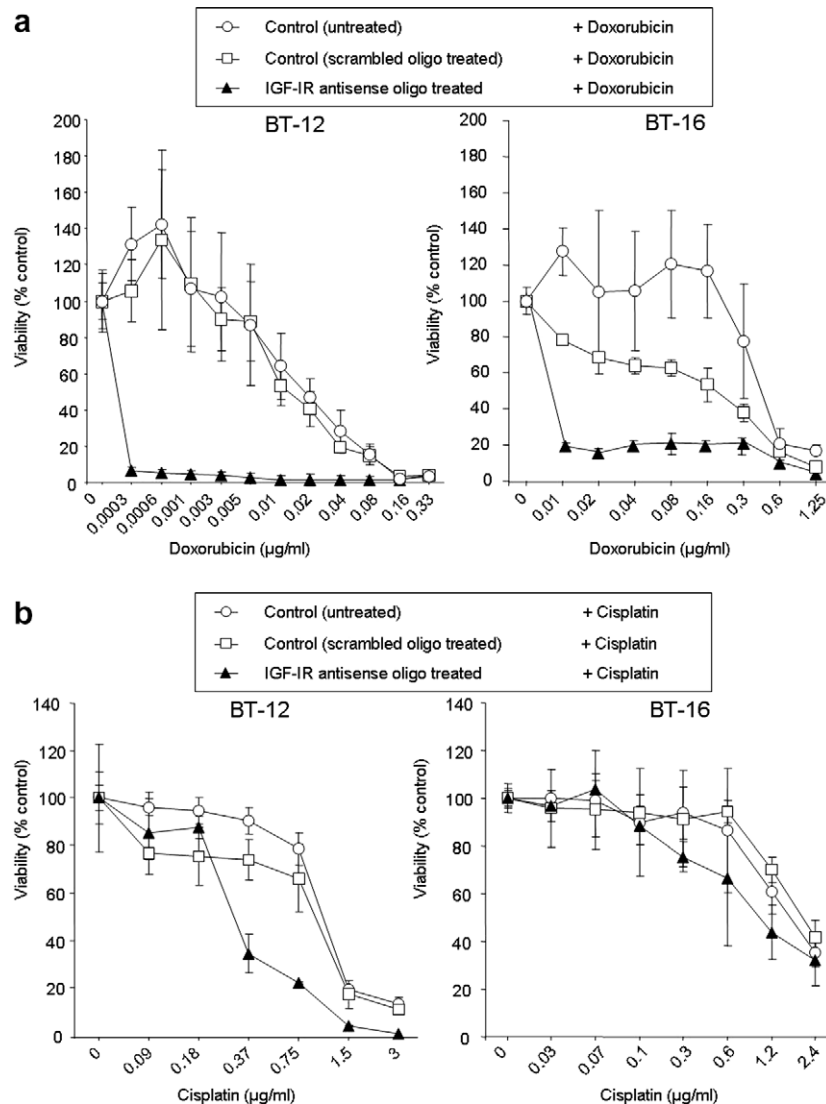


Fig. 6 – Down-regulation of IGF-IR through antisense oligonucleotide treatment (2 μ M; 48 h) results in significantly increased chemosensitivity of BT-12 and BT-16 human CNS AT/RT cells to doxorubicin (a), and cisplatin (b). Values represent the mean percentage of survival (\pm SD, $n = 3$) compared to a matched control which was not drug treated.

of chemosensitivity of BT-12 and BT-16 cells to doxorubicin (BT-12, IC-50: 0.0002 [95% confidence interval: 0.00009–0.00048] versus 0.015 [95% confidence interval: 0.0092–0.0231] $\mu\text{g/ml}$, $p < 0.0001$; BT-16, IC-50: 0.005 [95% confidence interval: 0.0016–0.0187] versus 0.11 [95% confidence interval: 0.0696–0.1767] $\mu\text{g/ml}$, $p < 0.0001$), and cisplatin (BT-12, IC-50: 0.325 [95% confidence interval: 0.2437–0.4338] versus 0.715 [95% confidence interval: 0.3744–1.367] $\mu\text{g/ml}$, $p = 0.017$; BT-16, IC-50: 1.05 [95% confidence interval: 0.8131–1.357] versus 2.00 [95% confidence interval: 1.632–2.457] $\mu\text{g/ml}$, $p = 0.001$).

4. Discussion

In the present study, we found a significant IGF-IR expression in all AT/RT specimen, as assessed by immunohistochemistry. Based on the analysis of two AT/RTs, for which material for Western blotting was available, the level of IGF-IR expression was found to be clearly over-expressed compared to normal brain and appeared to be higher when compared to other paediatric CNS neoplasms. Moreover, we found IGF-I and IGF-II mRNA in BT-16 human CNS AT/RT cells, and IGF-II mRNA in BT-12 human CNS AT/RT cells. In both cell lines, autophosphorylated IGF-IR was detected. Together with the results of Ogino et al.¹⁵ these results indicate the existence of an autocrine/paracrine IGF-I/II/IGF-IR loop in CNS AT/RT.

The binding of IGF-I and/or IGF-II to IGF-IR results in activation of its intrinsic tyrosine kinase with subsequent activation of the PI3 kinase-AKT-Bad cascade thereby protecting the cells from undergoing apoptosis.^{25,26} Activation of IGF-IR also suppresses pro-apoptotic pathways such as the JNK pathway.²⁷ It is therefore conceivable that highly expressed activated IGF-IR in CNS AT/RT might be involved in resistance to apoptosis. In agreement with this hypothesis is our finding that primary CNS AT/RT has a relatively high proliferation index, but only a low apoptotic index.

Recent studies demonstrate that the concept of IGF-IR targeting as an approach for growth control in specific tumour cells has qualified for the development of novel anti-cancer therapies (reviewed in [20,28]) Several strategies have been employed in different tumour cell lines to block either IGF-IR function or expression, both *in vitro* and *in vivo*. These included either inhibitors of ligand binding, e.g. peptide, small-molecule competitive binding antagonists and antireceptor antibodies or the use of inhibitors of IGF1R expression, such as siRNA and antisense (reviewed in [9]).

In the present study, we used antisense oligonucleotides to down-regulate IGF-IR in two human CNS AT/RT cell lines. We were able to demonstrate that IGF-IR mRNA and protein expression were significantly reduced in antisense oligonucleotide-treated cells compared to control cells.

IGF-IR down-regulation in CNS AT/RT cells resulted in a significant suppression of cellular proliferation, and induction of apoptosis. This is in accordance with previous *in vitro* findings in antisense oligonucleotide-mediated IGF-IR down-regulation in human lung cancer cells,²⁹ prostate cancer cells³⁰ and malignant glioma cells.³¹ Salatino et al. demonstrated inhibition of *in vivo* breast cancer growth by antisense oligonucleotides to IGF-IR mRNA.³²

We then studied whether down-regulation of IGF-IR alters chemosensitivity and found that treatment with IGF-IR antisense oligonucleotides resulted in a significant increase of sensitivity to doxorubicin and cisplatin. Our results are consistent with a large body of evidence which suggests that IGF-IR signalling results in chemotherapy resistance in a wide variety of tumours.³³ For instance, inhibition of IGF-IR signalling using a monoclonal antibody³⁴ or expression of a dominant-negative mutant of the IGF-IR³⁵ enhanced sensitivity to paclitaxel in breast cancer cell lines. An anti-IGF-IR antibody enhanced the sensitivity of pancreatic cancer xenografts to gemcitabine,³⁶ and antisense inhibition of IGF-IR enhanced sensitivity of prostate cancer cells to cisplatin, mitoxantrone and paclitaxel.³⁷

Taken together, our findings indicate that AT/RT express high levels of IGF-IR which may be activated through an autocrine/paracrine IGF-I/IGF-II/IGF-IR loop, contributing to the aggressiveness and therapy resistance of this particular paediatric brain tumour. Our results demonstrate that CNS AT/RT cell growth can be inhibited by treatment with IGF-IR antisense oligonucleotides. Moreover, we were able to demonstrate that antisense-mediated down-regulation of IGF-IR results in sensitisation to doxorubicin and cisplatin. These results raise the possibility that curability of selected tumours may be improved by pharmaceutical strategies directed towards the IGF-IR. The *in vivo* effects of IGF-IR inhibition and whether inhibition also influences the response of AT/RT cells to radiation therapy, are questions that remain to be answered.

Conflict of interest statement

None declared.

Acknowledgements

Supported by the Krebsliga Zürich and the Swiss Research Foundation Child and Cancer. We thank Prof. Dr. Burkhardt Seifert, Department of Biostatistics, University of Zurich, for assistance in statistical analysis.

REFERENCES

1. Rorke LB, Packer RJ, Biegel JA. Central nervous system atypical teratoid/rhabdoid tumours of infancy and childhood: definition of an entity. *J Neurosurg* 1996;**85**:56–65.
2. Judkins AR, Mauger J, Ht A, Rorke LB, Biegel JA. Immunohistochemical analysis of hSNF5/INI1 in pediatric CNS neoplasms. *Am J Surg Pathol* 2004;**28**:644–50.
3. Biegel JA, Tan L, Zhang F, Wainwright L, Russo P, Rorke LB. Alterations of the hSNF5/INI1 gene in central nervous system atypical teratoid/rhabdoid tumors and renal and extrarenal rhabdoid tumors. *Clin Cancer Res* 2002;**8**:3461–7.
4. Versteeg I, Sevenet N, Lange J, et al. Truncating mutations of hSNF5/INI1 in aggressive paediatric cancer. *Nature* 1998;**394**:203–6.
5. Burger PC, Yu IT, Tihan T, et al. Atypical teratoid/rhabdoid tumor of the central nervous system: a highly malignant tumor of infancy and childhood frequently mistaken for

- medulloblastoma: a Pediatric Oncology Group study. *Am J Surg Pathol* 1998;22:1083–92.
6. Bambakidis NC, Robinson S, Cohen M, Cohen AR. Atypical teratoid/rhabdoid tumors of the central nervous system: clinical, radiographic and pathologic features. *Pediatr Neurosurg* 2002;37:64–70.
 7. Hilden JM, Meerbaum S, Burger P, et al. Central nervous system atypical teratoid/rhabdoid tumor: results of therapy in children enrolled in a registry. *J Clin Oncol* 2004;22:2877–84.
 8. Tekautz TM, Fuller CE, Blaney S, et al. Atypical teratoid/rhabdoid tumors (ATRT): improved survival in children 3 years of age and older with radiation therapy and high-dose alkylator-based chemotherapy. *J Clin Oncol* 2005;23:1491–9.
 9. Pollak MN, Schernhammer ES, Hankinson SE. Insulin-like growth factors and neoplasia. *Nat Rev Cancer* 2004;4:505–18.
 10. Foulstone E, Prince S, Zaccheo O, et al. Insulin-like growth factor ligands, receptors, and binding proteins in cancer. *J Pathol* 2005;205:145–53.
 11. Antoniades HN, Galanopoulos T, Neville-Golden J, Maxwell M. Expression of insulin-like growth factors I and II and their receptor mRNAs in primary human astrocytomas and meningiomas; in vivo studies using in situ hybridization and immunocytochemistry. *Int J Cancer* 1992;50:215–22.
 12. Ogino S, Kubo S, Abdul-Karim FW, Cohen ML. Comparative immunohistochemical study of insulin-like growth factor II and insulin-like growth factor receptor type 1 in pediatric brain tumors. *Pediatr Dev Pathol* 2001;4:23–31.
 13. Del Valle L, Enam S, Lassak A, et al. Insulin-like growth factor I receptor activity in human medulloblastomas. *Clin Cancer Res* 2002;8:1822–30.
 14. Lichtor T, Kurpakus MA, Gurney ME. Expression of insulin-like growth factors and their receptors in human meningiomas. *J Neurooncol* 1993;17:183–90.
 15. Ogino S, Cohen ML, Abdul-Karim FW. Atypical teratoid/rhabdoid tumor of the CNS: cytopathology and immunohistochemistry of insulin-like growth factor-II, insulin-like growth factor receptor type 1, cathepsin D, and Ki-67. *Mod Pathol* 1999;12:379–85.
 16. Surmacz E. Growth factor receptors as therapeutic targets: strategies to inhibit the insulin-like growth factor I receptor. *Oncogene* 2003;22:6589–97.
 17. Turner BC, Haffty BG, Narayanan L, et al. Insulin-like growth factor-I receptor overexpression mediates cellular radioresistance and local breast cancer recurrence after lumpectomy and radiation. *Cancer Res* 1997;57:3079–83.
 18. Benini S, Manara MC, Baldini N, et al. Inhibition of insulin-like growth factor I receptor increases the antitumor activity of doxorubicin and vincristine against Ewing's sarcoma cells. *Clin Cancer Res* 2001;7:1790–7.
 19. Scotlandi K, Avnet S, Benini S, et al. Expression of an IGF-I receptor dominant negative mutant induces apoptosis, inhibits tumorigenesis and enhances chemosensitivity in Ewing's sarcoma cells. *Int J Cancer* 2002;101:11–6.
 20. Wang Y, Sun Y. Insulin-like growth factor receptor-1 as an anti-cancer target: blocking transformation and inducing apoptosis. *Curr Cancer Drug Targets* 2002;2:191–207.
 21. Zuzak TJ, Steinhoff DF, Sutton LN, Phillips PC, Eggert A, Grotzer MA. Loss of caspase-8 mRNA expression is common in childhood primitive neuroectodermal brain tumour/medulloblastoma. *Eur J Cancer* 2002;38:83–91.
 22. Bieche I, Nogues C, Paradis V, et al. Quantitation of hTERT gene expression in sporadic breast tumors with a real-time reverse transcription-polymerase chain reaction assay. *Clin Cancer Res* 2000;6:452–9.
 23. Axel DI, Spyridopoulos I, Riessen R, Runge H, Viebahn R, Karsch KR. Toxicity, uptake kinetics and efficacy of new transfection reagents: increase of oligonucleotide uptake. *J Vasc Res* 2000;37:221–34.
 24. Grotzer MA, Eggert A, Zuzak TJ, et al. Resistance to TRAIL-induced apoptosis in primitive neuroectodermal brain tumor cells correlates with a loss of caspase-8 expression. *Oncogene* 2000;19:4604–10.
 25. Datta SR, Dudek H, Tao X, et al. Akt phosphorylation of BAD couples survival signals to the cell-intrinsic death machinery. *Cell* 1997;91:231–41.
 26. Dudek H, Datta SR, Franke TF, et al. Regulation of neuronal survival by the serine-threonine protein kinase Akt. *Science* 1997;275:661–5.
 27. Okubo Y, Blakesley VA, Stannard B, Gutkind S, Le Roith D. Insulin-like growth factor-I inhibits the stress-activated protein kinase/c-Jun N-terminal kinase. *J Biol Chem* 1998;273:25961–6.
 28. Adachi Y, Lee CT, Carbone DP. Genetic blockade of the insulin-like growth factor 1 receptor for human malignancy. *Novartis Found Symp* 2004;262:177–89.
 29. Lee C-T, Wu S, Gabrilovich D, Chen H, et al. Antitumor effects of an adenovirus expressing antisense insulin-like growth factor I receptor on human lung cancer cell lines. *Cancer Res* 1996;56:3038–41.
 30. Burfeind P, Chernicky CL, Rininsland F, Ilan J. Antisense RNA to the type I insulin-like growth factor receptor suppresses tumor growth and prevents invasion by rat prostate cancer cells in vivo. *PNAS USA* 1996;93:7263–8.
 31. Andrews DW, Resnicoff M, Flanders AE, et al. Results of a pilot study involving the use of an antisense oligodeoxynucleotide directed against the insulin-like growth factor type I receptor in malignant astrocytomas. *J Clin Oncol* 2001;19:2189–200.
 32. Salatino M, Schillaci R, Proietti CJ, et al. Inhibition of in vivo breast cancer growth by antisense oligodeoxynucleotides to type I insulin-like growth factor receptor mRNA involves inactivation of ErbBs, PI-3K/Akt and p42/p44 MAPK signaling pathways but not modulation of progesterone receptor activity. *Oncogene* 2004;23:5161–74.
 33. LeRoith D, Helman L. The new kid on the block(ade) of the IGF-1 receptor. *Cancer Cell* 2004;5:201–2.
 34. Beech DJ, Parekh N, Pang Y. Insulin-like growth factor-I receptor antagonism results in increased cytotoxicity of breast cancer cells to doxorubicin and taxol. *Oncol Rep* 2001;8:325–9.
 35. Dunn SE, Ehrlich M, Sharp NJ, et al. A dominant negative mutant of the insulin-like growth factor-I receptor inhibits the adhesion, invasion, and metastasis of breast cancer. *Cancer Res* 1998;58:3353–61.
 36. Maloney EK, McLaughlin JL, Dagdigian NE, et al. An anti-insulin-like growth factor I receptor antibody that is a potent inhibitor of cancer cell proliferation. *Cancer Res* 2003;63:5073–83.
 37. Hellawell GO, Ferguson DJ, Brewster SF, Macaulay VM. Chemosensitization of human prostate cancer using antisense agents targeting the type 1 insulin-like growth factor receptor. *BJU Int* 2003;91:271–7.